# Prism lens for beam collimation in silicon photonic crystal beam-steering device

**Jun Maeda, Daichi Akiyama, Hiroyuki Ito, Hiroshi Abe, and Toshihiko Baba***

*Department of Electrical and Computer Engineering, Yokohama National University, 79-5 Tokiwadai, Hodogayaku, Yokohama 240-8501, Japan*
**Corresponding author: baba-toshihiko-zm@ynu.zc.jp*

Received XX Month XXXX; revised XX Month, XXXX; accepted XX Month XXXX; posted XX Month XXXX (Doc. ID XXXXX); published XX Month XXXX

**The doubly-periodic Si photonic crystal waveguide operates as a nonmechanical beam-steering device that can be applied to light detection and ranging. This study develops a prism lens that collimates a fan-shaped beam emitted from the waveguide independent of the steering angle. Its fundamental profile is investigated using theoretical analysis for thick lenses and then its detailed aspherical design is obtained. In ray tracing, this prism lens suppresses beam divergence to less than the diffraction limit in most of the targeted beam-steering range. The prism lens is fabricated by acrylic cutting and its expected characteristics are observed. © 2019 Optical Society of America**

http://dx.doi.org/10.1364/OL.99.099999

Over the past several years, light detection and ranging (LiDAR) devices have been extensively developed in the form of three-dimensional sensors for autonomous vehicles and robots [1, 2]. Conventional LiDAR devices have issues related to large size, low imaging speed, and high cost of assembly because they scan an optical beam using a mechanical steering device. As a solution to these problems, solid-state LiDAR devices based on a nonmechanical beam-steering device fabricated using Si photonics technology are attracting significant attention. Optical-phased arrays and waveguide diffraction gratings are candidates for nonmechanical beam-steering devices. However, the former has difficulties in integrating numerous optical antennas and precisely controlling their optical phases for a high-resolution beam, and the latter has issues with widely steering beams [3–10]. We have proposed and demonstrated a doubly-periodic Si photonic crystal waveguide (PCW) as an alternative, as shown in Fig. 1(a), which solves the problem of diffraction grating by means of the slow-light effect [11, 12]. This PCW beam-steering device consisting of a PCW with some kind of double periodicity emits a beam to free space with small divergence – full width at half maximum (FWHM $\delta\theta \sim 0.1°$) in direction $\theta$ along the PCW and wide divergence (FWHM $\delta\phi = 20°$–$40°$) in direction $\phi$ normal to the PCW. This fan-shaped beam is collimated using a lens to obtain a spot-like far-field pattern (FFP).

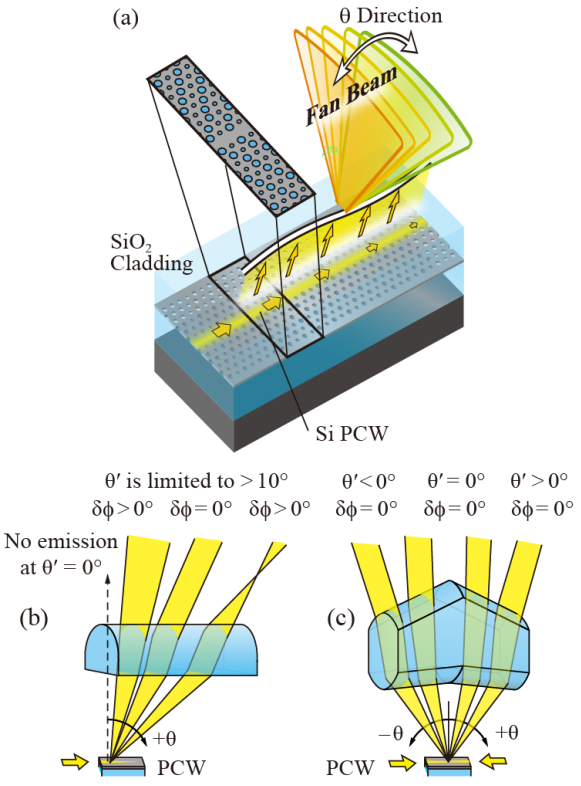


Fig. 1. Schematics of (a) single PCW beam steering device (arrayed configuration is not shown), (b) beam collimation using a cylindrical lens and (c) that using the proposed prism lens.

Then, steering in direction $\theta$ is obtained by changing wavelength $\lambda$ and/or PCW's refractive index $n_{PCW}$. The beam is also steered in direction $\phi$ by selecting one PCW from arrayed PCWs by

electrically controlling a set of 1 × 2 Mach-Zehnder thermo-optic switches integrated on the same chip, so that the PCW is offset against the collimator lens. The previous report described the use of a cylindrical lens like that in Fig. 1(b) [12]. For such a simple cylindrical lens, however, the larger the θ, the longer the distance from the PCW and the shorter the focal length when light obliquely enters the lens. Therefore, the collimation condition is only satisfied at a particular angle and not maintained for the wide range of θ. If the lens curvature is gradually changed in direction θ, the collimation condition may be maintained, while the FFP spot diverges in direction θ. In addition to this problem, vertical emission at θ = 0° cannot be obtained because it is the Bragg condition of the doubly-periodic PCW, in which a standing wave is formed in the PCW and the FFP of the emission disappears due to destructive interference. These problems constrain the applications of this device.

This paper proposes and demonstrates a prism lens, as illustrated in Fig. 1(c), in order to solve these issues. This lens comprises two different-curvature convex lenses formed on the upper and lower surfaces of the prism. The angles of these surfaces and the curvature are particularly designed so that the collimation condition becomes insensitive to θ and the beam angle θ is converted to θ′ including vertical direction. In addition, it is proposed to switch the direction of light incidence on the PCW to utilize both positive and negative θ, resulting in two times wider beam-steering range. Therefore, the prism lens is shaped to be bilaterally symmetric. This study investigated the fundamental profile of the prism lens using optic analysis for thick lenses, which rendered its detailed design using ray tracing. Furthermore, it was fabricated using acrylic cutting and its collimation characteristics have been observed.

This study considered a doubly-periodic PCW wherein a guided mode is gradually emitted into free space and attenuated gradually. A standard PCW structure was assumed to be operating at a wavelength λ = 1.55 μm [13], with a waveguide length of 1.2 mm, a radiation coefficient of 100 dB/cm (= 23 $cm^{-1}$), a propagation loss of 35 dB/cm (= 8 $cm^{-1}$), and an effective aperture length that attenuates the guided mode intensity to $1/e$ of 311 μm. When λ and $n_{PCW}$ are changed, the beam is steered in the range of θ = 0°–30° at maximum (θ = −30°–30° using bilateral light incidence). As mentioned earlier, however, the emission efficiency of light drops around θ = 0°. Therefore, the effective range θ = 10°– 30° (θ′ = 0°–20°) was assumed (although in reality, it was slightly wider than this range). The refractive index of the lens was set at $n_{lens}$ = 1.48, considering an acrylic resin at λ = 1.55 μm and that of surroundings $n_{air}$ = 1.0. The prism profile was first fixed so that it converts θ = 10° into θ′ = 0°, and the center angle $\theta_0$ = 20° ($\theta_0'$ = 10°) satisfies the condition of the minimum deviation angle at which the corresponding ray in the prism lens is parallel to the bottom of the prism. Figure 1(b) shows an example structure, where the slope angles of upper and lower surfaces against the horizontal plane are 24.6° and 5.5°, respectively, meaning that the angle between two surfaces is 2ϕ = 19.1°.

The structural parameters of the prism lens are defined as shown in Fig. 2(a). The curvature radii of the lenses on upper and lower surfaces are denoted as the functions of $\theta_0$ as $R_1$, and $R_2$, respectively. The collimation condition for a fan beam is then given from a well-known condition for thick lenses [14] as

$$\frac{(n_{lens}-1)l_1}{R_1} = \frac{1-\dfrac{(n_{lens}-1)l_2}{n_{lens}R_2}}{1+\dfrac{R_1}{R_2}-\dfrac{(n_{lens}-1)l_2}{n_{lens}R_2}}, \quad (1)$$

where $l_1$ is the distance between the PCW and lens, and $l_2$ is the lens thickness on the ray. Next, it is considered that θ is changed to $\theta_0 \pm \Delta\theta$; then variations occur such that $l_1 \to l_1 \pm \Delta l_1$, $l_2 \to l_2 \mp \Delta l_2$, $R_1 \to R_1 \mp \Delta R_1$, and $R_2 \to R_2 \pm \Delta R_2$ due to the profile. These were substituted into Eq. (1), and subsequently set as $R_1 = R_2 = R_0$ and $\Delta R_1 = \Delta R_2 = \Delta R$ for simplicity. The following is obtained by neglecting high-order terms:

$$\Delta l_1 = \frac{\dfrac{l_2}{4n_{lens}}}{1-\dfrac{(n_{lens}-1)l_2}{2n_{lens}R_0}}\left(\frac{\dfrac{\Delta l_2}{l_2}}{1-\dfrac{(n_{lens}-1)l_2}{2n_{lens}R_0}}-\frac{2\Delta R}{R_0}\right). \quad (2)$$

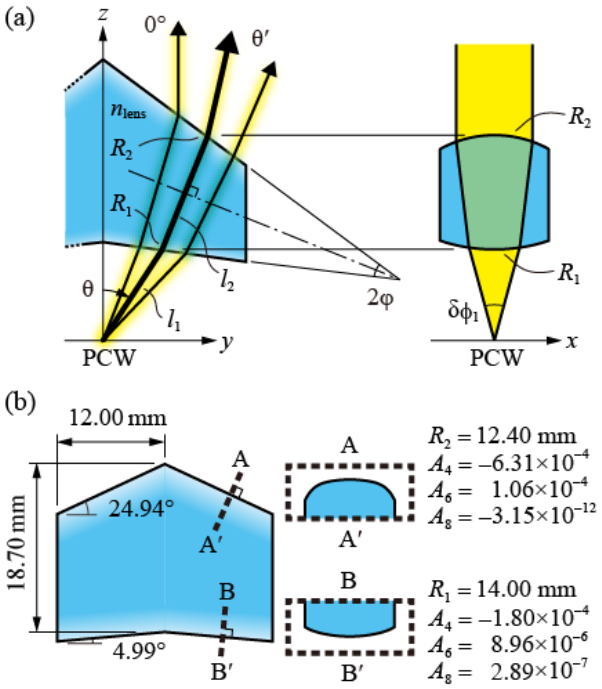


Fig. 2. Prism lens design. (a) Parameters in the side view (left figure) and front view (right figure). (b) Example design of prism lens used for fabrication in acrylic resin.

The collimation condition is maintained when this equation holds, and the parameters that satisfy it can be actually found. Since high-order terms are neglected, the error increases when Δθ is too large. In addition, this analysis assumed a point light source, while light is emitted from the PCW over the aperture length in direction $y$, meaning that this condition is not completely satisfied. However, when the prism lens is sufficiently larger than the aperture length in the $y$ direction, the collimation condition in Eq. (2) is approximately satisfied.

The initial parameters were determined so as to satisfy Eq. (2). Ray tracing was then performed using a commercial software, CYBERNET Light Tools, assuming a fan beam calculated for the doubly-periodic PCW as the light source. First, a moderate value of $R_0$ was set, and the collimation condition was obtained at $\theta_0$. Then, the optimal aspherical shapes of lenses were identified using an optimization tool from Light Tools. Figure 2(b) shows an example design where the aspherical function is expressed by the following equation, including 4th–8th order aspherical constants $A_4$–$A_8$, which were finally determined by searching optimum values using Light Tools:

$$z = \frac{x^2/R_i}{1+\sqrt{1-x^2/R_i}} + A_4x^4 + A_6x^6 + A_8x^8 \quad (i = 1, 2) \quad , \qquad (3)$$

The beam spot diagram obtained by ray tracing in the range of $|\theta| = 10°–40°$ and $|\phi| \le 10°$ is shown in Fig. 3; (a) is for a plano-convex lens (Thorlabs, LJ1878L2-C, $f = 10.0$ mm), and (b) is for the designed prism lens. For simulating light output from the PCW, we assumed a planar light source of 1.2mm in direction $x$ and 1 μm, in direction $y$ with $\delta\theta = 0°$. Regarding $\delta\phi$, we also assumed a quadratic variation between $\delta\phi = 44.9°–16.8°$ for $\theta = 10°–30°$, respectively, which were calculated by a finite-difference time-domain simulation, and set $\delta\phi = 16.8°$ in the range of $\theta = 30°–40°$ just for drawing this spot diagram, because the light output from the PCW is not actually obtained due to the restriction of light line that radiates the guided slow-light mode into the $SiO_2$ claddings. The plano-convex lens certainly cannot output a spot at $|\theta'| \le 10°$ because of the absence of angle conversion. In this calculation, the collimation condition was set at $|\theta| = 20°$. When $|\theta|$ is apart from this angle, the spot severely diverges in direction $\phi$. For the designed prism lens, on the other hand, continuous steering is expected in the range of $|\theta'| \le 20°$ due to angle conversion. The divergence $\delta\theta$ and $\delta\phi$ both increase when $|\theta'|$ becomes larger than 20°. But in the device's effective range of $|\theta'| \le 20°$ and $|\phi'| \le 5°$, these divergence values are, in most cases, smaller than 0.05°, which is smaller than the diffraction limit of the actual device estimated using wave analysis. When the light source is offset in direction $x$ for beam steering in direction $\phi$, the spot most diverges at $|\theta'| = 0°$ and $|\phi'| = 5°$ but still its divergence is $\delta\phi = 0.12°$.

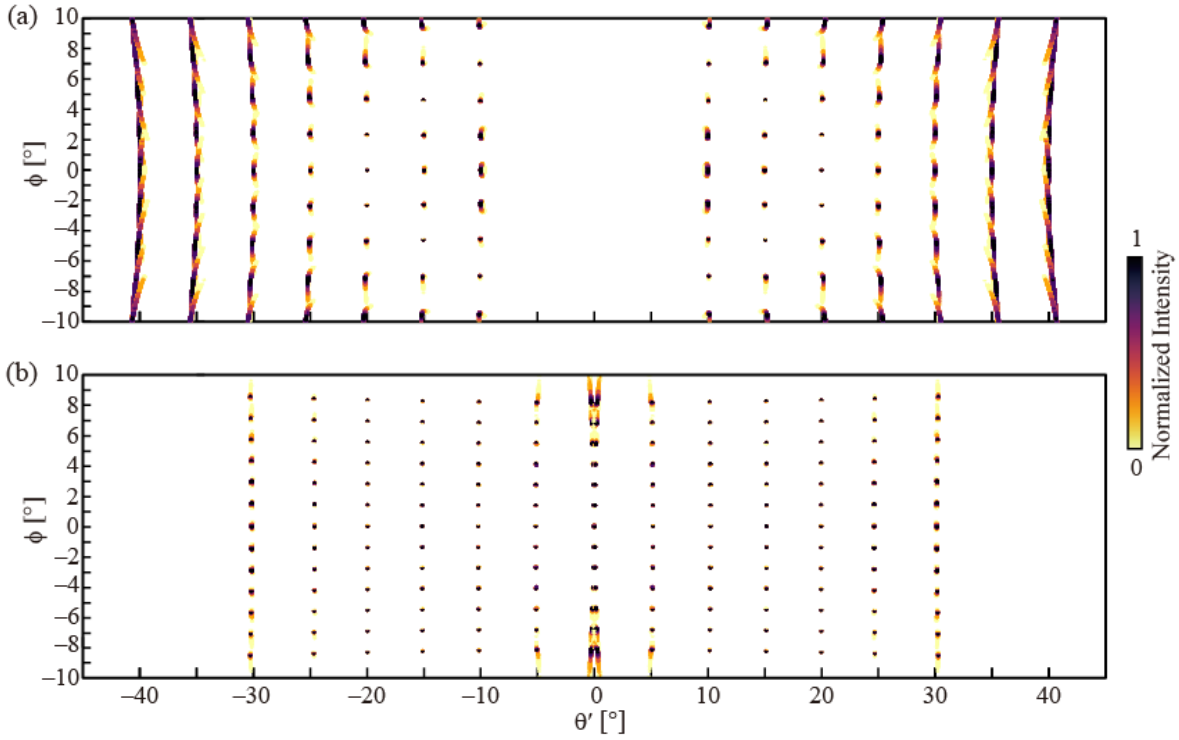


Fig. 3 Beam spot diagram of (a) plano-convex lens and (b) designed aspherical prism lens, which were obtained by ray tracing.

The designed prism lens was fabricated by cutting acrylic resin. Figure 4(a) shows the side view of the prism lens and PCW chip in an optical measurement setup. Laser light was launched into the PCW via the fiber lens module and endfire spotsize converter; the fan beam emitted upward was collimated using either a plano-convex lens (Thorlabs, LJ1310L2-C, $f = 4.0$ mm) or the prism lens, and it was observed with a far-field microscope with an InGaAs camera (Raptor, OWL1280). Figure 4(b) and (c) show FFPs at $\lambda =$ 1518 – 1535 nm. The plano-convex lens was aligned so that the beam was collimated at $\theta = \theta' = 18°$. Then, $\delta\phi$ was increased to 1°–2° when $\theta$ was changed. The prism lens was aligned so that the beam was collimated at $\theta = 20°$, $\theta' = 10°$. Then, $\delta\phi$ was less than 0.1° at $-2° < \theta' < 22°$, which was the full emission range of the used PCW.

In summary, we developed the prism lens that collimates the fan-shaped beam from the PCW as a nonmechanical beam-steering device that is unaffected by the beam angle change. We designed the fundamental profile of the prism lens using optic analysis and obtained a detailed design using ray tracing. The ray tracing shows

that the beam divergence is less than the diffraction limit that is calculated by wave analysis for an actual device, in the most beam-steering range of $|\theta| \le 20°$ and $|\phi| \le 5°$; the worst $\delta\phi$ is 0.12° in the limited range. We also fabricated the prism lens and observed the expected beam collimation characteristics. Such collimation characteristics are considered to be unavailable by a standard single lens or may require a complicated lens unit. The size of the prism lens is enlarged by compensating errors caused by the long emission aperture; if the aperture is short, the lens can be miniaturized and the steering range in direction $\phi$ is enhanced. Anyway, this prism lens is crucial in developing a nonmechanical slow-light LiDAR device, but we also expect it to be also useful for other applications.

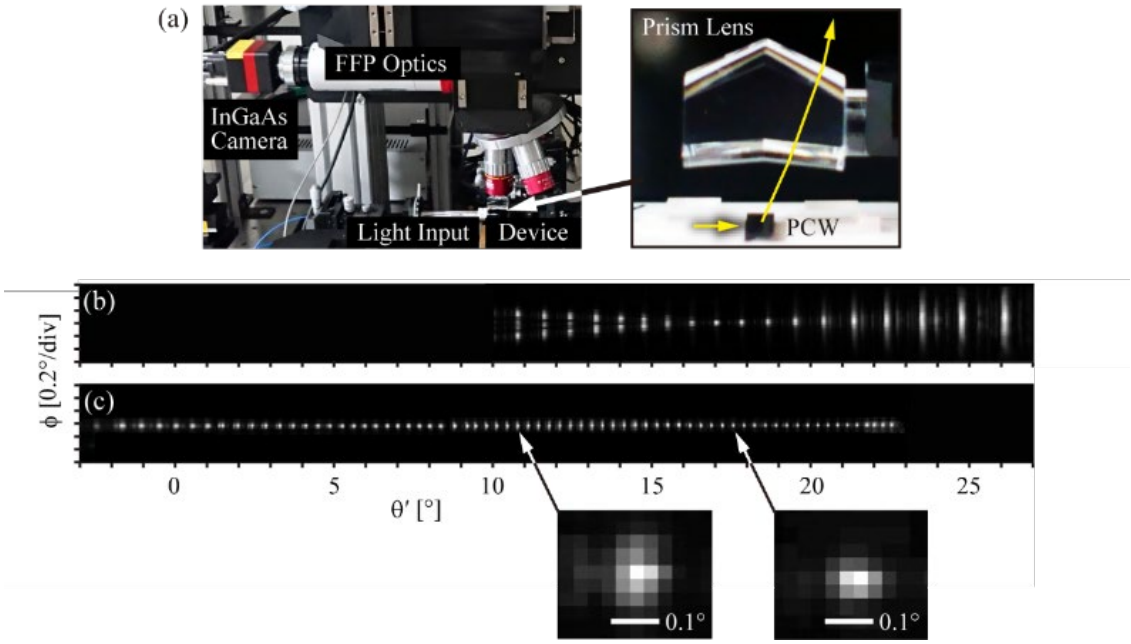


Fig. 4 (a) Fabricated prism lens with PCW in the optical measurement setup. (b) FFP of collimated beam observed for plano-convex lens when $\lambda$ is shifted with a wavelength step of 1 nm. (c) The designed prism lens with a wavelength step of 0.5 nm.

**Funding.** Innovation Research Initiative Turning Top Science and Ideas into High-Impact Values (ACCEL): Japan Science and Technology Agency (JST) (JPMJAC1603).

**Disclosures.** The authors declare that there are no conflicts of interest related to this article.

## References

1. T. T. Sankey, J. McVay, T. L. Swetnam, M. P. McClaran, P. Heilman, and M. Nichols, Remote Sensing in Ecology and Conservation **4**, 20 (2018).
2. K. Ito, C. Niclass, I. Aoyagi, H. Matsubara, M. Soga, S. Kato, M. Maeda, and M. Kagami, IEEE Photonics J. **5**, 6800114 (2013).
3. K. Van Acoleyen, H. Rogier, and R. Baets, Opt. Express **18**, 13655 (2010).
4. J. K. Doylend, M. J. R. Heck, J. T. Bovington, J. D. Peters, L. A. Coldren, and J. E. Bowers, Opt. Express **19**, 21595 (2011).
5. J. Sun, A. Yaacobi, E. Timurdogan, Z. Su, D. B. Cole, E. Hosseini, M. Moresco, G. Leake, D. Coolbaugh, and M. R. Watts, IEEE J. Sel. Top. Quantum Electron. **20**, 8201115 (2014).
6. D. Kwong, A. Hosseini, J. Covey, Y. Zhang, X. Xu, H. Subbaraman, and R. T. Chen, Opt. Lett. **39**, 941 (2014).
7. H. Abediasl and H. Hashemi, Opt. Express **23**, 6509 (2015).
8. D. N. Hutchison, J. Sun, J. K. Doylend, R. Kumar, J. Heck, W. Kim, C. T. Phare, A. Feshali, and H. Rong, Optica **3**, 887 (2016).
9. M. Zadka, Y.-C. Chang, A. Monhanty, C. T. Phare, S. P. Roberts, and M. Lipson, Opt. Express **26**, 2528 (2018).
10. C. V. Poulton, M. J. Byrd, P. Russo, E. Timurdogan, M. Khandaker, D. Vermeulen, and M. R. Watts, IEEE J. Sel. Topics Quantum Electron., **25**, 7700108 (2019).
11. H. Abe, M. Takeuchi, G. Takeuchi, H. Ito, T. Yokokawa, K. Kondo, Y. Furukado, and T. Baba, Opt. Express **26**, 9389 (2018).
12. Y. Furukado, H. Abe, Y. Hinakura and T. Baba, Opt. Express **26**, 18222 (2018).
13. G. Takeuchi, Y. Terada, M. Takeuchi, H. Abe, H. Ito and T. Baba, Opt. Express **26**, 11529 (2018).
14. J. E. Greivenkamp, *Field Guide to Geometrical Optics* (SPIE PRESS, 2004).

## Full references


1. T. T. Sankey, J. McVay, T. L. Swetnam, M. P. McClaran, P. Heilman, and M. Nichols, "UAV hyperspectral and lidar data and their fusion for arid and semi-arid land vegetation monitoring," Remote Sensing in Ecology and Conservation **4**(1), 20–33 (2018).
2. K. Ito, C. Niclass, I. Aoyagi, H. Matsubara, M. Soga, S. Kato, M. Maeda, and M. Kagami, "System design and performance characterization of a MEMS-based laser scanning time-of-flight sensor based on a 25664-pixel single-photon imager," IEEE Photonics J. **5**(2), 6800114 (2013).
3. K. Van Acoleyen, H. Rogier, and R. Baets, "Two-dimensional optical phased array antenna on silicon-oninsulator," Opt. Express **18**(13), 13655–13660 (2010).
4. J. K. Doylend, M. J. R. Heck, J. T. Bovington, J. D. Peters, L. A. Coldren, and J. E. Bowers, "Two-dimensional free-space beam steering with an optical phased array on silicon-on-insulator," Opt. Express **19**(22), 21595–21604 (2011).
5. J. Sun, A. Yaacobi, E. Timurdogan, Z. Su, D. B. Cole, E. Hosseini, M. Moresco, G. Leake, D. Coolbaugh, and M. R. Watts, "Large-scale integrated silicon photonic circuits for optical phased arrays," IEEE J. Sel. Top. Quantum Electron. **20**(4), 8201115 (2014).
6. D. Kwong, A. Hosseini, J. Covey, Y. Zhang, X. Xu, H. Subbaraman, and R. T. Chen, "On-chip silicon optical phased array for two-dimensional beam steering," Opt. Lett. **39**(4), 941–944 (2014).
7. H. Abediasl and H. Hashemi, "Monolithic optical phased-array transceiver in a standard SOI CMOS process," Opt. Express **23**(5), 6509–6519 (2015).
8. D. N. Hutchison, J. Sun, J. K. Doylend, R. Kumar, J. Heck, W. Kim, C. T. Phare, A. Feshali, and H. Rong, "High-resolution aliasing-free optical beam steering," Optica **3**(8), 887 (2016).
9. M. Zadka, Y.-C. Chang, A. Monhanty, C. T. Phare, S. P. Roberts, and M. Lipson, "On-chip platform for a phased array with minimal beam divergence and wide field-of-view," Opt. Express **26**(3), 2528-2534 (2018).
10. C. V. Poulton, M. J. Byrd, P. Russo, E. Timurdogan, M. Khandaker, D. Vermeulen, and M. R. Watts, "Long-range LiDAR and free-space data communication with high-performance optical phased arrays," IEEE J. Sel. Topics Quantum Electron., **25**(5), 7700108 (2019).
11. H. Abe, M. Takeuchi, G. Takeuchi, H. Ito, T. Yokokawa, K. Kondo, Y. Furukado, and T. Baba, "Two-dimensional beam-steering device using a doubly periodic Si photonic-crystal waveguide," Opt. Express **26**(8), 9389-9397 (2018).
12. Y. Furukado, H. Abe, Y. Hinakura and T. Baba, "Experimental simulation of ranging action using Si photonic crystal modulator and optical antenna," Opt. Express **26**(14), 18222-18229 (2018).
13. G. Takeuchi, Y. Terada, M. Takeuchi, H. Abe, H. Ito and T. Baba, "Thermally controlled Si photonic crystal slow light waveguide beam steering device," Opt. Express **26**(9), 11529-11537 (2018).
14. J. E. Greivenkamp, *Field Guide to Geometrical Optics* (SPIE PRESS, 2004).